Present-day uplift patterns over Greenland from a coupled ice-sheet/visco-elastic bedrock model

E. Le Meur[1]

Alfred-Wegener-Institut für Polar- und Meeresforschung, Bremerhaven, Germany

P. Huybrechts[2]

Departement Geografie, Vrije Universiteit Brussel, Brussel, Belgium

Abstract. We present results from a fully coupled ice/bedrock model calculation of the Greenland ice sheet and the underlying Earth during the last two glacial cycles. The method treats the mutual interaction between the ice and the bedrock and yields the main glacial-isostatic characteristics of the ice-sheet evolution and the bedrock adjustment since the Last Glacial Maximum. By taking advantage of the splitting of the present-day rate of bed uplift into a viscous and an elastic component, these results allow one to distinguish between the bedrock response to the past and present ice sheet evolution, respectively.

Introduction

The bedrock response under large ice caps needs to be accounted for when modelling evolving ice sheets because it couples with the ice dynamics. This is evident from the effect bedrock changes have on ice-sheet surface elevation, and consequently, on surface temperature and melting. Previous studies [*Le Meur and Huybrechts*, 1996; *Tarasov and Peltier*, 1997] show how different ways of treating isostasy can influence these dynamics and also demonstrate the necessity for accurate Earth representations. Our approach combines a self-gravitating spherical visco-elastic model [*Le Meur*, 1996b; *Peltier*, 1974; *Wu and Peltier*, 1982; *Spada et al.*, 1992] with a 3-D thermomechanical ice-sheet model in a simulation over Greenland. The quality of the results follows from the fact that the ice-sheet model has been successfully tested against a variety of Greenland field data, including on the chronology of the last glacial-interglacial transition [*Huybrechts et al.*, 1991; *Huybrechts*, 1994; *Van Tatenhove et al.*, 1995], and the fact that the bedrock model has given satisfactory results when compared with the Fennoscandian post-glacial rebound data set [*Le Meur*, 1996a].

Following a brief description of both models, the coupling describes how the ice-sheet and bedrock models interact and simulate the Ice/Earth dynamics. Time-dependent as well as geometrical features of the surface displacement are depicted and are shown to be consistent with what can be expected according to the past and present ice-sheet evolution. The splitting into a long-term viscous part driven by

the past loading history and an elastic instantaneous component related to the current load change offers an interesting possibility for inferring the present-day ice-sheet evolution.
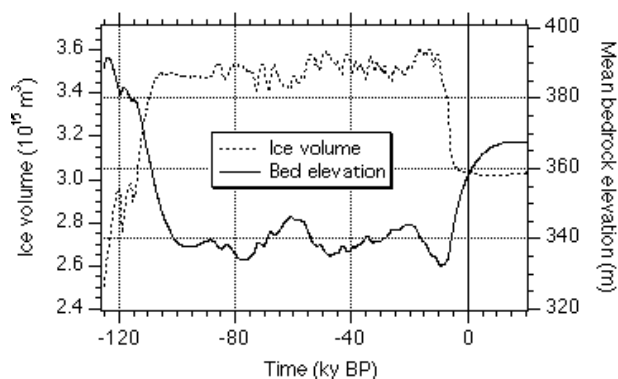
Description of the Models

The Bedrock Model

The bedrock model [*Le Meur*, 1996a, b] belongs to the well-known category of self gravitating spherical visco-elastic Earth models [*Peltier*, 1974; *Wu and Peltier*, 1982; *Lambeck et al.*, 1990; *Spada et al.*, 1992]. Following the work of *Spada et al.* [1992], the model has been coded into a semi-analytical form using the symbolic algebra manipulator Mathematica. We adopted an Earth structure comprising an inviscid core (between the center up to 3480 km), a visco-elastic mantle (3480-6271 km) and a purely elastic lithosphere (the upper 100 km) which is here assumed to be compressible. The three viscous mantle layers consist of a 2.10^{21} Pa.s lower mantle (from the core mantle boundary up to 670 km deep), overlain by a 1.10^{21} Pa.s upper mantle with an outermost low viscosity zone (between 420 km and 100 km deep) of 5.10^{20} Pa.s, which are each approximated by the appropriate Maxwell solid. The unit impulse (both in time and space) as a means of forcing the model gives rise to the impulse response Love numbers whose convolution with the appropriate time-space function allows the treatment of any kind of loading scenario.

The Ice Sheet Model

The time-dependent ice-dynamics model [*Huybrechts et al.*, 1991; *Huybrechts*, 1996] solves the full thermomechani-
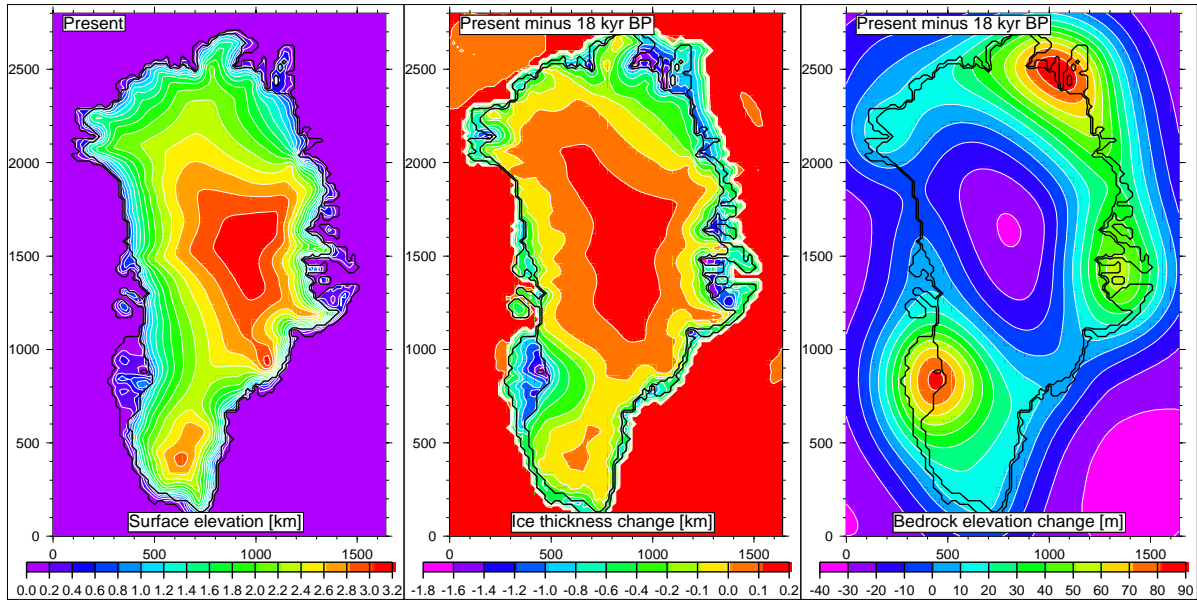
---

[1]Now at British Antarctic Survey, Cambridge, UK

[2]Also at Alfred-Wegener-insitut für Polar- und Meeresforschung, Bremerhaven, Germany

Figure 1. Time-dependent total ice volume and mean bedrock elevation during the last glacial cycle.

Figure 2. Present ice-sheet topography, ice thickness change and the resulting bedrock displacement since 18 kyr BP (the patches at sea correspond to water loading changes).

cal equations for ice flow on a three-dimensional mesh and includes basal sliding as well as heat conduction in the underlying bedrock. The rate factor in Glen's flow law depends on both the ice temperature and the age of the ice. The flow and temperature calculations are made on a numerical grid with a horizontal resolution of 20 km and 31 layers in the vertical. By including a sea-level forcing and the possibility of extension over the continental shelf during periods of lower sea-level, the model is able to freely generate the ice-sheet geometry in response to a prescribed distribution of surface mass-balance and surface temperature. The mass-balance model distinguishes between snow accumulation, rainfall, superimposed ice formation, and runoff, which components are all parameterised in terms of temperature. In this experiment, the model is driven by a prescribed temperature change from the recent GRIP δ^{18}O record and by the SPECMAP sea-level record, both at a 100 year resolution. The calculations span all of the two last glacial cycles (the last 225 000 years) to eliminate the effects of the choice of the initial conditions.

Coupling of the two Models

The coupling consists first in forcing the bedrock model with the loading from the ice model. With these loading data, the bedrock model computes the corresponding new bedrock topography which is then reinserted in the ice model so that the effects of bedrock changes on the ice dynamics can be fully accounted for. The viscous part of the current bedrock response is by more than 99 % determined by the loading history over the last 30 kyrs. The discrete time-integration over this period of the viscous Love numbers arising from the impulse model (a viscous displacement amplitude $h_n^j(a)$ and the inverse of a decaying period $1/s_n^j$ for each of the 4 main viscous modes) with a 100 yr (Δt) time-step therefore gives $N_m - 1$ elementary contributions $G_{n,k}(a)$ (with $N_m = 30000yrs/\Delta t = 300$). So defined,

$G_{n,k}(a) = \sum_{j=1}^{4} \frac{h_n^j(a)}{s_n^j} [e^{s_n^j(N_m-k)\Delta t} - e^{s_n^j(N_m-k-1)\Delta t}]$ represents the radial viscous displacement in response to the unit load that prevailed between $(N_m-k-1)\Delta t$ and $(N_m-k)\Delta t$ before the current time t. Each of these contributions is then weighted by the corresponding load difference between the time considered and the reference state $L_{i_1,j_1}(k)$ at the (i_1,j_1) point before being summed over time from $k = 1$ to $k = N_m - 1$ as shown in eq. 1. To incorporate the regional character of the bedrock response, the grid over which the loads are calculated is extended beyond the 83 x 141 ice-sheet model grid by a radius of influence set to 1000 km. As a consequence, not only the ice loading (ice density times the local ice thickness H_{i_1,j_1}), but also the water loading (sea-water density times the water column) are considered, thereby enabling the incorporation of the effects of sea level changes. The elastic contribution only implies one elastic surface Love number amplitude $h_n^E(a)$ (asymptotic limit of the general model solution when inverting the Laplace transform, see *Wu and Peltier*, [1982]) and the current state of loading $L_{i_1,j_1}(N_m)$.

The spatial convolution for each (i,j) point of the numerical grid incorporates the contribution to deformation of all the neighbouring (i_1,j_1) points within the radius of influence $D_{i,j}$. The colatitudinal dependence of the total bedrock response (viscous + elastic) is obtained by summing a Legendre series up to an harmonic cut off set at $N_{max} = 200$, in which $P_n(\cos\theta_{i,i_1,j,j_1})$ represents the Legendre polynomial and θ_{i,i_1,j,j_1} the angle at the surface of the Earth between (i_1,j_1) and (i,j)). Since each grid point has its own time history, the time and space convolutions cannot be split. This gives for the surface radial displacement R at node (i,j) and time t :

$$R_{ij}(t) = \sum_{i_1,j_1 \in D_{i,j}} \Big[\sum_{n=0}^{200} \frac{a}{M_e} \Big(\sum_{k=1}^{N_m-1} L_{i_1,j_1}(k)\, G_{n,k}(a) + L_{i_1,j_1}(N_m)\, h_n^E(a) \Big) P_n(\cos\theta_{i,i_1,j,j_1}) \Big] \Delta x \Delta y \qquad (1)$$
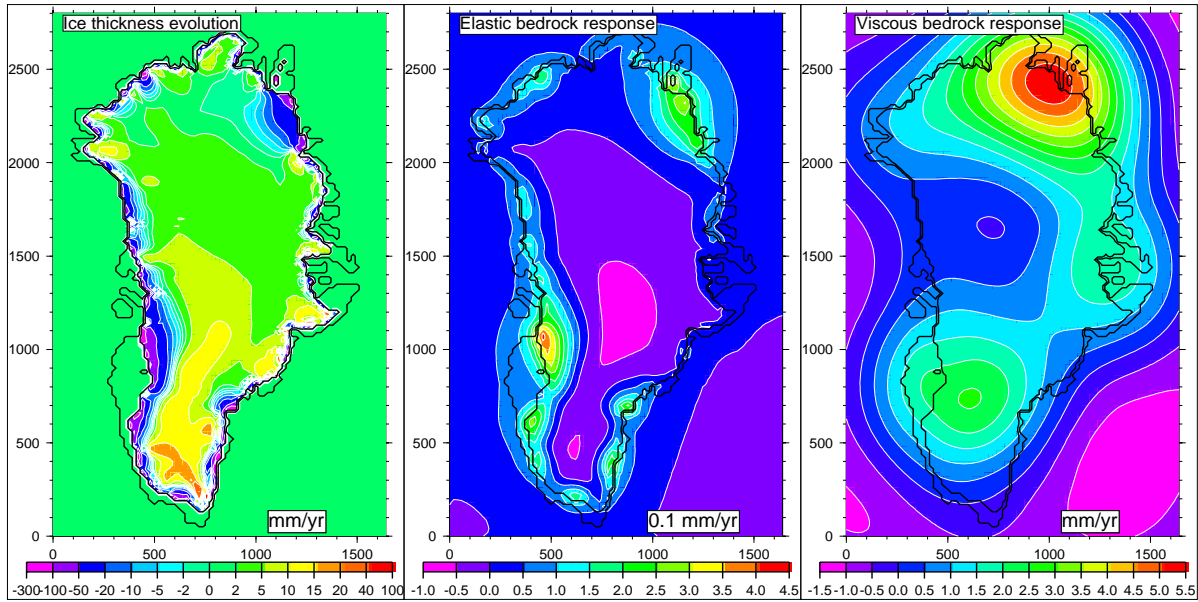
Figure 3. Present-day ice thickness changes as averaged over the last 200 years, corresponding elastic bedrock response and the long-term viscous bedrock response.

in which a/M_e is the Earth's radius/mass ratio resulting from the dimensionless Love numbers [*Wu and Peltier*, 1982] and Δx, Δy are the x and y grid spacings (20 km for both).

Results of the Simulation

The simultaneous evolution of total ice volume and mean bedrock height for the last 125000 are displayed in Figure 1. They appear to be well correlated during the slow built-up phase, though the bedrock uplift displays a time lag of a few thousand years in response to the recent faster deglaciation. This non-linearity is a direct consequence of the discrepancy between the long time constant of the viscous mantle and the fast evolving load of a decaying ice sheet. As the Earth viscous response is a function of the past loading events, an ongoing future evolution of the mean bedrock elevation occurs despite an almost constant load (rightmost part of Figure 1).

Figure 2 shows a clear correspondence between the deglaciated areas since the Last Glacial Maximum and the total corresponding uplift. The similarity is affected by the rigid behavior of the lithosphere, which acts as a low-pass filter and makes the response regional instead of local. Therefore, the result is a smoothed imprint of the loading change pattern which consists of both a discontinuous peripheral deglaciation belt, especially in the southwest and northeast of Greenland, and a central thickening of the ice sheet.

Calculating the uplift rate requires a different version of eq. 1 in which the loading function L is replaced by its time derivative in the elastic part and by the finite difference formula $\frac{(L(k+1)-L(k))}{\Delta t}$ for the viscous part. The definition of the time period to calculate the present-day ice thickness change (dL/dt) remains however ambiguous. Theoretically, it is the real instantaneous change occuring at time t, but for numerical-technical reasons (time step in calculations, discontinuous forcing), the ice sheet model cannot yield a meaningful instantaneous imbalance. Moreover, in reality, the relevance of the instantaneous imbalance is questionable

because a strong interannual to decadal variability in the surface mass balance (precipitation minus ablation) generally overrides a more significant longer-term ice-sheet dynamic imbalance. We follow here the same approach as in *Huybrechts* [1994], and average the model outputs over the last 200 years to obtain the present evolution (Figure 3). This assumption is justified as the elastic response of the lithosphere involves microphysical processes that probably need several years or even decades to complete. Such a period can still be considered as instantaneous when compared to the characteristic times for the viscous response.

The total present-day change of Greenland ice volume is predicted to be close to zero. This confirms the basic result obtained in *Huybrechts* [1994] which was furthermore shown to be very robust to changes in ice-dynamic parameters. Despite this near overall equilibrium, the geographical pattern of ice thickness changes shows a clear distinction between a thickening of between 0 and +20 mm/ yr over the accumulation zone and thinning rates locally in excess of 100 mm/ yr at the southwestern and northeastern margins of the ice sheet (Figure 3, left panel). A comparison between these current ice thickness changes and the elastic bedrock response indicates a less regional response pattern than for the viscous part. This is because over the short periods characteristic of the elastic response, the asthenosphere (viscous response) does not have time to react and prevents the plate from bending. The elastic deformation therefore reduces to a more local compression or relaxation, proportional to the load variations as the lithosphere is assumed to be compressible. When, on the other hand, we consider the long-term viscous response (Figure 3, right panel), the outflow of mantle material allows the upperlying lithosphere to bend with a more pronounced regional character owing to the rigid stiffness of the plate. In terms of amplitude, the elastic instantaneous response remains small compared to the viscous response with a maximum elastic uplift of less than 0.5 mm/ yr compared to a maximum viscous response of about 6 mm/ yr. The main consequence of this difference

is that the total present-day rate of uplift mainly depends upon past loading events rather than on the present changes of the ice sheet.

Conclusion

This study has shown the importance of the viscous long-term component in the present-day Earth isostatic response over Greenland. The elastic part appears much smaller but remains quite speculative as are the present-day ice loading changes necessary to compute it. One solution to this problem could come from reliable field data for bedrock level changes [*Wahr et al.*, 1995]. Indeed, by substracting the modelled viscous term, such data should be able to provide an independent assessment of the more problematic elastic term. This justifies the fully coupled approach adopted in this paper, which offers a comprehensive way to obtain the viscous term. Moreover, if the spatial coverage of these field data is wide and dense enough, the possibility of deconvolving the inferred bedrock elastic term might help in constraining the present-day ice imbalance, at least for the ice sheet margin. The recent GPS campaigns over the ice-free areas are very promising in this respect, but the main question is whether they have been carried out for long enough to produce reliable trends. The much older ground gravity surveys (though certainly less dense), on the other hand, probably fulfill this last requirement, meaning that a similar approach but with the gravity anomaly is worth investigating.

References

Huybrechts, P., The present evolution of the Greenland ice sheet: an assessment by modelling, *Global and Planetary Change 9,* 39-51, 1994.

Huybrechts, P., Basal temperature conditions of the Greenland ice sheet during the glacial cycles, *Ann. Glaciol. 23,* 226-236, 1996.

Huybrechts, P., A. Letreguilly, and N. Reeh, The Greenland ice sheet and greenhouse warming, *Palaeogeogr., Palaeoclimatol., Palaeoecol. 89,* 399-412, 1991.

Lambeck, K., P. Johnston, and M. Nakada, Holocene glacial rebound and sea-level change in NW Europe, *Geophys. J. Int. 103,* 451-468, 1990.

Le Meur, E., Isostatic post-glacial rebound over Fennoscandia with a self-gravitating spherical visco-elastic Earth model, *Annal. Glaciol. 23,* 318-327, 1996a.

Le Meur E., Spécificité de l'isostasie en contexte glaciaire. Présentation et et application d'un modèle de réponse terrestre, PhD. thesis, Université Joseph Fourier - Grenoble I, 325 pp., 1996b.

Le Meur, E. and P. Huybrechts, A comparison of different ways of dealing with isostasy: examples from modelling the Antarctic ice sheet during the last glacial cycle, *Annal. Glaciol. 23,* 309-317, 1996.

Peltier, W. R., The impulse response of a Maxwell Earth, *Rev. Geophys. Space Phys. 12,* 649-669, 1974.

Spada, G., R. Sabadini, D. A. Yuen, and Y. Ricard, Effects on post-glacial rebound from the hard rheology in the transition zone, *Geophys. J. Int. 109,* 683-700, 1992.

Tarasov, L. and W. R. Peltier, A High-Resolution Model of the 100 kyr Ice-Age Cycle, *Ann. Glaciol. 25,* 58-65, 1997.

Van Tatenhove, F. G. M., J. J. M. Van der Meer, and P. Huybrechts, Glacial-geological/geomorphological research in West Greenland used to test an ice-sheet model, *Quaternary Research 44,* 317-327, 1995.

Wahr, J., D. Han and A. Trupin, Prediction of vertical uplift caused by changing polar ice volumes on a viscoelastic earth, *Geophys. Res. Lett. 22,* 977-980, 1995.

Wu, P. and W. R. Peltier, Viscous gravitational relaxation, *Geophys. J, R. astr. Soc. 70(2),* 4335-485, 1982.

P. Huybrechts, Departement Geografie, Vrije Universiteit Brussel, Pleinlaan 2, B-1050 Brussel, Belgium. (e-mail: phuybrec@vub.ac.be)

E. Le Meur, British Antarctic Survey, High Cross, Madingley Road, CB3 0ET Cambridge, UK. (e-mail: lemeur@mail.nerc-bas.ac.uk)